J Supercond Nov Magn (2015) 28:2697–2702
DOI 10.1007/s10948-015-3101-y

ORIGINAL PAPER

Temperature-modulated Growth of MOCVD-derived $YBa_2Cu_3O_{7-x}$ Films on IBAD-MgO Templates

Fei Zhang[1] · Jie Xiong[1] · Ruipeng Zhao[1] · Yan Xue[1] · Hui Wang[2] · Qiuliang Wang[2] · Yuanying He[1] · Pan Zhang[1] · Bowan Tao[1]

Received: 3 March 2015 / Accepted: 6 May 2015 / Published online: 28 May 2015

Abstract The cost-effective and environment-friendly template of $LaMnO_3$/epi-MgO/ion beam-assisted deposited (IBAD-)MgO/solution deposition planarized (SDP) Y_2O_3/Hastelloy tape was used as the substrate, on which the technique of metal organic chemical vapor deposition (MOCVD) has been applied to depositing 1.2-μm-thick $YBa_2Cu_3O_{7-x}$(YBCO) films by modulating the substrate temperature ranging from 750 to 850 °C. The effects of substrate temperature on the preferential orientation, textures, surface morphology, and performance of the YBCO films were systematically investigated. X-ray diffraction and scanning electron microscope revealed that as substrate temperature increased from 750 to 810 °C, the orientation of YBCO films was transferred from the *a*-axis to the *c*-axis; meanwhile, the textures were improved and the films became denser. However, as the substrate temperature rose above 810 °C, the composition distributions and textures of YBCO films degraded quickly, and the films were barium-poor with $CuYO_2$ impurity arising, of which all negatively affected the critical current density (J_c) of YBCO films. Around 810 °C, the YBCO film was of the best crystallization and microstructure as well as highly epitaxial growth, leading to the highest $J_c$of 1.8 MA/cm^2 at 77 K and self-field.

Keywords MOCVD · YBCO · Substrate temperature · IBAD · SDP

1 Introduction

Owing to its large current capacity and high irreversible field, the second generation high-temperature superconducting (HTS) $YBa_2Cu_3O_{7-x}$ (YBCO) tape, also called YBCO-coated conductor (CC), is of wide prospection to be used in electric power field, such as current transmission cables, transformers, motors, and electromagnets [1, 2]. The YBCO CC is composed of flexible metal substrate, buffer layer, YBCO layer, and protective layer from bottom to top. The YBCO CC with high performance requires the YBCO layer should be highly textured [3]. Up to now, there are following two mainstream routes to obtain textures for YBCO CC: the rolling-assisted biaxially textured substrate (RABiTS) and the ion beam-assisted deposition (IBAD) texturing [4, 5]. Compared to RABiTS, IBAD technique is cost-effective and the finally obtained YBCC CC is of higher performance, even though its structure is more complex [6, 7].

Nowadays, the typical templates applying IBAD technique are the following: $LaMnO_3$/homo-epi MgO/IBAD-MgO/Y_2O_3/Al_2O_3/Hastelloy tape and PLD-CeO_2/IBAD-MgO/Y_2O_3/Al_2O_3/Hastelloy tape [6, 8]. In order to get superior template for high-performance YBCO CC, smooth surface with average surface roughness of ∼ 1 nm is

✉ Jie Xiong
jiexiong@uestc.edu.cn; zfchunri@gmail.com

[1] State Key Laboratory of Electronic Thin Film and Integrated Devices, University of Electronic Science and Technology of China, Chengdu, 610054 People's Republic of China

[2] Applied Research Laboratory of Superconduction and New Material, Institute of Electric al Engineering, Chinese Academy of Sciences, Beijing, 100190 People's Republic of China

necessary through several methods for planarizing Hastelloy tape, such as electrochemical or mechanical polishing, unfortunately, which is cost-expensive and environmentally harmful [9, 10]. Moreover, the Y_2O_3 and Al_2O_3 usually are deposited by the vacuum coating technique, which would somewhat increase the fabricating cost. An alternative method, solution deposition planarization (SDP) process using multiple chemical solution coatings of Y_2O_3 with a total thickness of approximately 1 μm [10] is developed not only to planarize the tape but also to provide the effective barrier layer replacing of amorphous Y_2O_3 and Al_2O_3.

Considering its easy composition adjustment, relatively low vacuum requirement and high throughput for the deposition of YBCO films as well as its mature application in semiconductor industry [6], the metal-organic chemical vapor deposition (MOCVD) has become one of the main techniques to fabricate YBCO CCs. Unfortunately, the MOCVD growth of multi-element oxide thin films is difficult to control due to the reciprocal effect among the temperature, compositions, and impurity phases.

In this paper, MOCVD was used to fabricate YBCO films on simple, cost-effective SDP-based templates of $LaMnO_3$ /homo-epi MgO/IBAD-MgO/SDP-Y_2O_3/Hastelloy tape, and the effects of substrate temperature on the evolvement of the microstructures and superconducting properties of YBCO films were investigated.

2 Experimental Details

In the experiments, a custom-built MOCVD system was applied to depositing YBCO films on home-made IBAD-MgO templates of $LaMnO_3$/homo-epi MgO/IBAD-MgO/SDP-Y_2O_3/Hastelloy tape [11, 12]. The metal-organic solids of $Y(tmhd)_3$, $Ba(tmhd)_2$, and $Cu(tmhd)_2$ (tmhd: 2,2,6,6,-tetramethyl-3,5-heptanedionate) were dissolved into tetrahydrofuran (THF) by the concentration of 0.063, 0.133, and 0.163 mol/L, respectively, to form a mixed liquid precursor. Such liquid precursor was evaporated to gas, which then was transported by the carrier of argon and mixed with the reactive gas of oxygen and N_2O. Finally, the mixed gas showered to the preheated IBAD-MgO templates to form YBCO films. The preset temperature of IBAD-MgO templates were 750 to 850 °C by the interval of 20 °C and the corresponding deposition rate was ∼ 600 nm/min. Finally, the as-formed YBCO films were annealed at 500 °C for 40 min in the atmosphere of 1 bar O_2 to be transferred into superconducting phase. More details about the deposition could be found elsewhere [11].

The texture of the as-fabricated YBCO films was examined by X-ray diffraction (XRD, Bede D1 system). The surface microstructure was characterized by scanning electron microscope (SEM, JEOL7500F). The film thickness was obtained by step profiler (Veeco Dektak 150). And the critical current density J_c at 77 K and self-field was measured through nondestructive induction method by Leipzig J_c-scan system [13].

3 Results and Discussion

The as-deposited YBCO films were 1.2-μm-thick and the corresponding XRD θ-2θ scans were showed in Fig. 1. At the lower substrate temperature (T_s) of 750 °C, there are clear peaks of YBCO(*00l*) and (*h00*), which means the *a*-axis- and *c*-axis-oriented YBCO grains coexisted in the film. Meanwhile, the peak intensity of YBCO (200) is relatively strong and comparable to that of YBCO(006), indicating that there are considerable volume of the *a*-axis-oriented grains in the film. As T_s increases to 770 °C, the peak intensity of YBCO(200) decreases a lot, while the peak intensity of YBCO(*00l*) becomes stronger, revealing that the growth mode of YBCO film is gradually transferring from the partially *a*-axis-oriented growth to the fully *c*-axis-oriented growth as T_s increases. When T_s is in the range from 790 to 850 °C, there are only (*00l*) peaks of YBCO, indicating that the YBCO films fabricated at such T_s are completely *c*-axis oriented. However, the intensity of (*00l*) peaks become stronger at $T_s$of 790∼ 810 °C, then weaker at $T_s$of 810∼ 850 °C. Around T_s of 810 °C, the YBCO(*00l*) peaks are most sharp and intense, implying that the YBCO film crystallizes best and is of the best *c*-axis epitaxial growth. As $T_s$increases from 810 to 850 °C, the intensities of (*00l*) peaks decline dramatically, attributed to the deteriorated texture and nonstoichiometric composition, which is proved by the presence of impurity phase of $CuYO_2$.

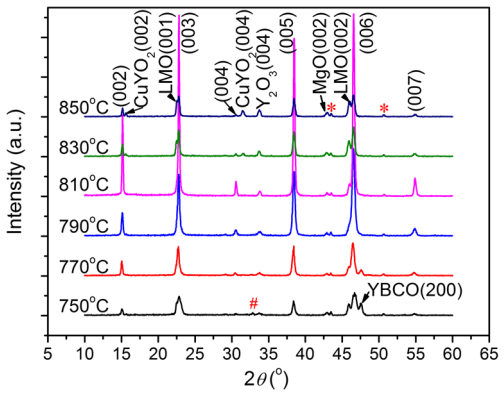

Fig. 1 The XRD θ-2θ scans of YBCO films deposited at substrate temperature of 750, 770, 790, 810, 830, and 850 °C. The *asterisk* and *number symbols* represent peaks of Hastelloy metal and YBCO(103), respectively

It is worth noting that the peaks of Y_2O_3(004) appear in the θ-2θ patterns of all the YBCO films and becomes stronger as T_s increases. This diffraction peak of Y_2O_3(004), although the work to identify the origin is in progress, is likely from the Y_2O_3 grains precipitated during the YBCO film deposition or the crystallization of the amorphous SDP-Y_2O_3 because of the high deposition temperature of MOCVD-YBCO film. Then, on the one hand, the Y_2O_3 precipitates are helpful in improving the flux pinning [14, 15]. On the other hand, however, the crystallization of the amorphous SDP-Y_2O_3 may lead to the formation of grain boundaries which are the main diffusion passage of oxygen elements and transition metal elements [16], thus may result in the oxidization of Hastelloy tape and the diffusion of metal elements into YBCO layer, ultimately deteriorating the mechanical and superconducting properties of the YBCO. Replacing Y_2O_3 with Y_2O_3-Al_2O_3 composite [17] can be a way to avoid the crystallization of the amorphous SDP-Y_2O_3.

To further demonstrate the evolvement of the film orientation and crystallization with T_s increasing, XRD χ-scan [18] has been performed on YBCO(102). The χ-scan patterns were depicted in Fig. 2, in which peaks located around 33.4° and 56.6° represented the *a*-axis- and *c*-axis-oriented YBCO grains, respectively. It is apparent that the peak around 33.4° declines and then disappears with T_s increasing, while the peak around 56.6° rises first and then drops. To give a quantitative study on the content of the *a*-axis component, the value $I_a = I_a(102)/(I_c(102) + I_a(102))$, where $I_a(102)$ and $I_c(102)$ are the integrated intensities of peaks around 33.4° and 56.6°, respectively, is used. $I_a$values at 750 and 770 °C are 58.1 and 14.2 %, respectively, and are zero above 790 °C, which means that the YBCO film transfers its growth mode from the *a*-axis dominated to the *c*-axis dominated as T_s increases from 750 to 850 °C, which is consistent with that in Fig. 1.

XRD ω-scan and ϕ-scan have been performed on YBCO(005) and YBCO(103), respectively, to examine the out-of-plane and in-plane textures. The full width at half maximum (FWHM, $\Delta\omega$ or $\Delta\phi$) values determined by the ω-scans and ϕ-scans were plotted in Fig. 3, and the smaller FWHM value corresponds to the better texture. Figure 3 shows that the textures of YBCO film are strongly affected by T_s, especially the out-of-plane textures. At T_s = 810 °C, the $\Delta\omega$ of 1.4° and $\Delta\phi$ of 3.0° are the smallest, corresponding to the best out-of-plane and in-plane texture, which is comparable to those reported in ref. [17]. The inset in Fig. 3 is the pole figure of YBCO(103) and shows that there are four 90° spaced peaks, which implies that the YBCO prepared at 810 °C was single-domain epitaxial without misoriented grains. As T_s is further away from 810 °C, the FWHM value becomes larger, meaning that the texture of YBCO film became worse.

It is known that during film formation, there are following basic processes: atom adsorption and condensation, diffusion, nucleation, island formation and growth, and coalescence, which are strongly affected by T_s. At the lower T_s of 750 °C, the atoms could not receive enough energy from substrate, yielding that the YBCO film tended to grow along the easy growth orientation of the *a*-axis and was hybrid of the *a*-axis and *c*-axis grains. As T_s is increased from 750 to 810 °C, the adsorbed atoms could gain more energy from substrate, thereby adjust their position to minimize the free energy. YBCO film texture was improved and the best was achieved at 810 °C. When T_s further increased from 810 to 850 °C, the surface diffusion was so severe that the smaller nuclei could move with a greater distance to coalesce with larger nuclei. The larger nuclei annexed the smaller nuclei and continued to grow up so fast that there remained

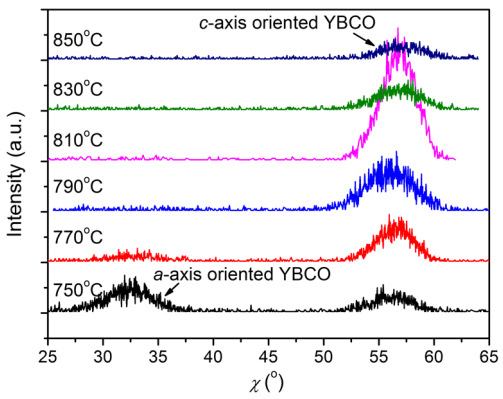

Fig. 2 The XRD χ−scans on (102) planes of YBCO films deposited at substrate temperature of 750, 770, 790, 810, 830, and 850 °C

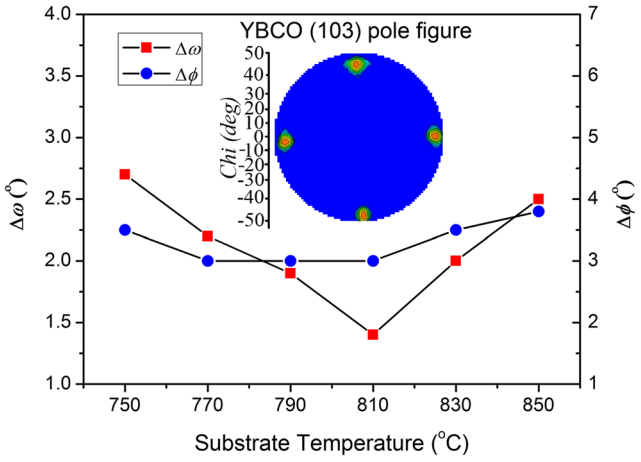

Fig. 3 The substrate-temperature dependence of FWHM values of ω-scans on YBCO(005) and ϕ-scans on YBCO(103)

insufficient time for them to be preferentially oriented. Moreover, the excessive T_s made the film barium-poor, demonstrated by the formation of the $CuYO_2$ impurity denoted in Fig. 1. The large lattice mismatch between YBCO and $CuYO_2$ would yield enormous strain in the system. Because of the above facts, the intensities of YBCO(*00l*) peaks declined and the FWHM values increased, meaning that the film crystallization and textures deteriorated.

The SEM was employed to get a comprehensive picture about the microstructure of the film. The corresponding images are showed in Fig. 4, in which the needle-like phases were the *a*-axis YBCO grains. Figure 4a shows the morphology of the film formed at 750 °C, indicating that the typical *a*-axis grains cover the whole film surface and pinholes are clearly visible [18]. As T_s increases, the numbers of *a*-axis grains and holes decrease, while the average grain size increases as shown in Fig. 4b–f. It should be noted that bright and dark regions start to appear on the surface at 810 °C, implying that the film becomes inhomogeneous in composition as T_s is increased beyond 810 °C.

The J_c(77 K, 0 T) values of all films were summarized in Fig. 5. It is obvious that J_c increased from 0.2 to 1.8 MA/cm^2 as T_s increased from 750 to 810 °C. It was reported that J_c of the *a*-axis films was only 2–3 % to that

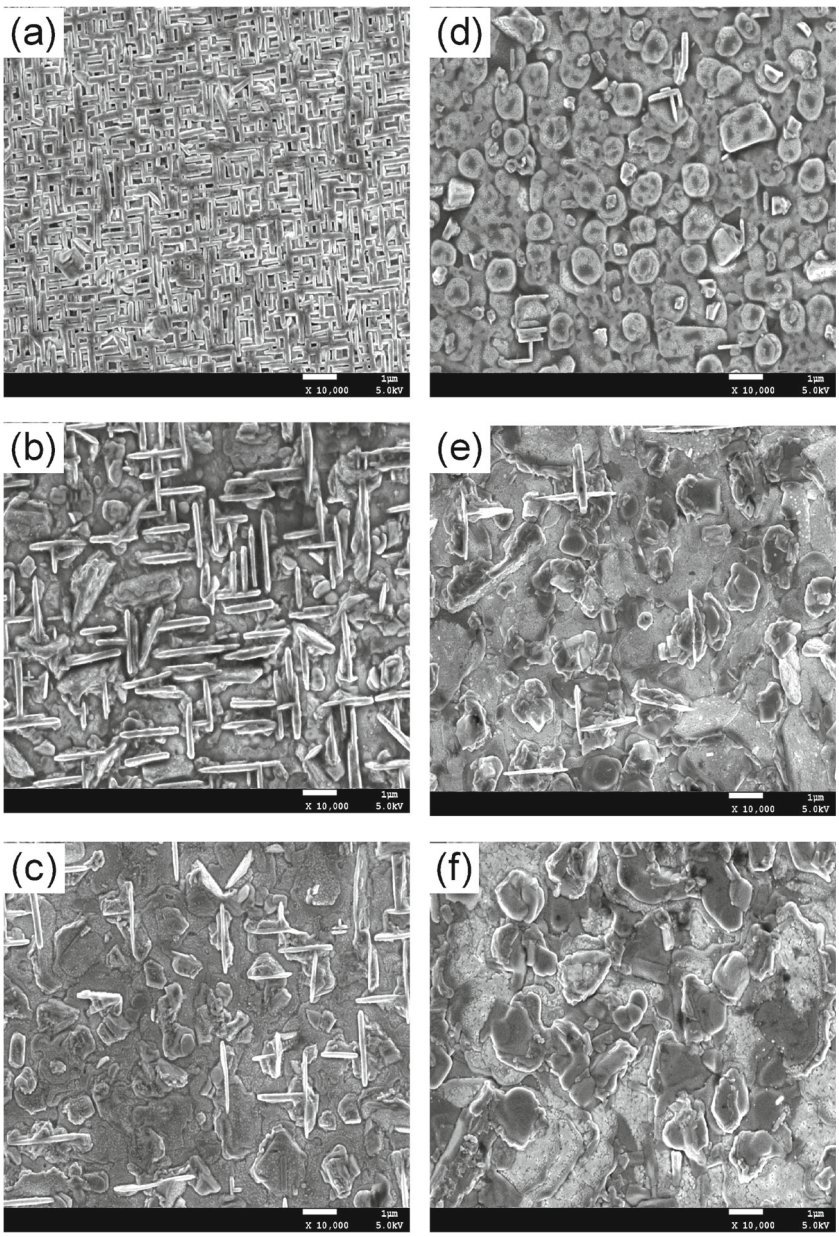

Fig. 4 SEM images of YBCO films deposited at different substrate temperature: **a** 750,; 770; **c** 790,; 810, ; 830; **f** 850 °C

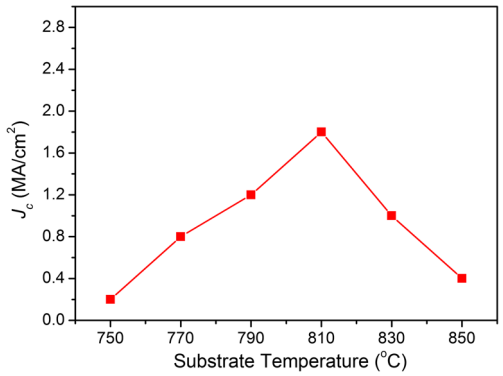

Fig. 5 The relationship between J_c(77 K, 0 T) of YBCO films and the substrate temperature

of the *c*-axis film, and the worse textures mean more large-angle grain boundaries which were harmful to supercurrent transportation [3, 19, 20]. Hence, such J_c enhancement was benefited from the above-discussed decrease of the *a*-axis grains and improvement of texture and continuity of YBCO film. As T_s increased to 850 °C, the J_c declined from 1.8 to 0.4 MA/cm^2, which was attributed to the degraded texture, inhomogeneous composition, and emergence of $CuYO_2$ impurities, which was consistent with the above XRD results. Although the yielded maximum J_c of 1.8 MA/cm^2 at present is smaller than those of YBCO films reported in refs. [21–24], yet it is expected to improve the J_c by further adjusting the process parameters of MOCVD-YBCO deposition, such as total pressure of the chamber, partial pressure of oxygen and N_2O, and atom ratio of the metal elements in precursor.

4 Conclusions

The substrate temperature is important to determine the preferential orientation and textures of YBCO film. We have demonstrated the feasibility of using a simple, cost-effective SDP-based IBAD-MgO template for YBCO-coated conductors, and investigated the evolvement of the microstructures and superconducting properties of YBCO films by tuning the substrate temperature. At lower substrate temperature of 750 °C, the film growth was dominated by the *a*-axis aligned mode, which severely deteriorated the superconducting property. As T_s increased from 750 to 810 °C, the films transferred their preferential orientation from the *a*-axis to the *c*-axis, and the in-plane and out-of-plane textures of the films were remarkably improved. Benefiting from the decrease of the *a*-axis grains and improvement of the textures, the J_c was greatly ameliorated from 0.2 to 1.8 MA/cm^2. Further enhanced temperature would degrade the film texturing and lead to inhomogeneous composition and barium-poor.

Acknowledgments We gratefully acknowledge the support of the National Science Foundation of China under Grant No. 91421110, National Basic Research Program (973) of China through Grant No. 2015CB358600, Sichuan Youth Science and Technology Innovation Research Team Funding (No.2011JTD0006), and the Fundamental Research Funds for the Central Universities (No.ZYGX2011Z002) for this work.

Conflict of interests The authors declare that they have no competing interest.

Research Involving Human Participants and/or Animals
This research has not involved any human participants and animals.

Informed Consent

All authors listed in the manuscript have been involved in the research and also have been informed with the ethical responsibilities. They are clear with the results in this paper and agree to submit it to be published after having acquired the consent of the responsible authorities.

References

1. Malozemoff, A.P., Verebelyi, D.T., Fleshler, S., Aized, D., Yu, D.: HTS wire: status and prospects. Phys. C **386**, 424–430 (2003)
2. Jin, J.X., Xin, Y., Wang, Q.L., He, Y.S., Cai, C.B., Wang, Y.S., Wang, Z.M.: Enabling high-temperature superconducting technologies toward practical applications. IEEE Trans. Appl. Supercond. **24**, 5400712 (2014)
3. Durrell, J.H., Rutter, N.A.: Importance of low-angle grain boundaries in $YBa_2Cu_3O_{7-\delta}$ coated conductors. Supercond. Sci. Technol. **22**, 013001 (2009)
4. Goyal, A., Norton, D.P., Budai, J.D., et al.: High critical current density superconducting tapes by epitaxial deposition of $YBa_2Cu_3O_x$ thick films on biaxially textured metals. Appl. Phys. Lett. **69**, 1795–1797 (1996)
5. Iijima, Y., Tanabe, N., Kohno, O., Ikeno, Y.: In-plane aligned $YBa_2Cu_3O_{7-x}$ thin films deposited on polycrystalline metallic substrates. Appl. Phys. Lett. **60**, 769–771 (1992)
6. Xie, Y.Y., Selvamanickam, V., Marchevsky, M., Chen, Y.M., Xiong, X.M., Rar, A., Lenseth, K., Qiao, Y.F., Hazelton, D., Knoll, A., Dackow, J.: Second-generation HTS wire manufacturing and technology advancement at SuperPower, Applied Superconductivity and Electromagnetic Devices, 2009. ASEMD 2009. International Conference on doi:10.1109/ASEMD.2009.5306613
7. Rupich, M.W., Li, X.P., Sathyamurthy, S., Thieme, C.L.H., DeMoranville, K., Gannon, J., Fleshler, S.: Second generation wire development at AMSC. IEEE Trans. Appl. Supercond. **23**, 6601205 (2013)
8. Igarashi, M., Kakimoto, K., Hanyui, S., Kikutake, R., Sutoh, Y., Suzuki, R., Daibo, M., Fuji, H., Kutami, H., Iijima, Y., Itoh, M., Saitoh, T.: Advanced development of IBAD/PLD coated conductors at FUJIKURA. Phys. Proc. **36**, 1412–1416 (2012)
9. Xie, Y.Y., Knoll, A., Chen, Y., et al.: Progress in scale-up of second-generation high-temperature superconductors at SuperPower Inc. Phys. C **426-431**, 849–857 (2005)
10. Sheehan, C., Jung, Y., Holesinger, T., Feldmann, D.M., Edney, C., Ihlefeld, J.F., Clem, P.G., Matias, V.: Solution deposition planarization of long-length flexible substrates. Appl. Phys. Lett. **98**, 071907 (2011)

11. Zhang, F., Xiong, J., Liu, X., Zhao, R.P., Zhao, X.H., Tao, B.W., Li, Y.R.: Double-sided reel-to-reel metal-organic chemical vapor deposition system of $YBa_2Cu_3O_{7-\delta}$ thin films. J. Vac. Sci. Technol. A **32**, 041512 (2014)
12. Xiong, J., Xue, Y., Xia, Y.D., Zhang, F., Zhang, Y.X., Li, L.H., Zhao, X.H., Tao, B.W.: Fabrication of long-length ion beam-assisted deposited MgO templates for YBCO-coated conductors. Rare Met. **32**(6), 574–578 (2013)
13. Hochmuth, H., Lorenz, M.: Side-selective and non-destructive determination of the critical current density of double-sided superconducting thin films. Phys. C **265**, 335–340 (1996)
14. Song, X.Y., Chen, Z.J., Kim, S., Feldmann, D.M., Larbalestier, D., Reeves, J., Xie, Y.Y., Selvamanickam, V.: Evidence for strong flux pinning by small, dense nanoprecipitates in a Sm-doped $YBa_2Cu_3O_{7-\delta}$ coated conductor. Appl. Phys. Lett. **88**, 212508 (2006)
15. Chen, Y.M., Selvamanickam, V., Zhang, Y.F., Zuev, Y., Cantoni, C., Specht, E., Paranthaman, M.P., Aytug, T., Goyal, A., Lee, D.: Enhanced flux pinning by $BaZrO_3$ and (Gd, Y)$_2O_3$ nanostructures in metal organic chemical vapor deposited GdYBCO high temperature superconductor tapes. Appl. Phys. Lett. **94**, 062513 (2009)
16. Tsukuia, S., Koritala, R.E., Li, M., Goretta, K.C., Adachi, M., Baker, J.E., Routbor, J.L.: Oxygen and cation diffusion in YBCO coated conductors. Phys. C **392-396**, 841–846 (2003)
17. Stan, L., Feldmann, D.M., Usov, I.O., Holesinger, T.G., Maiorov, B., Civale, L., DePaula, R.F., Dowden, P.C., Jia, Q.X.: Composite Y_2O_3-Al_2O_3 as diffusion barrier/nucleation layer for HTS coated conductors based on IBAD MgO. IEEE Trans. Appl. Supercond. **19**, 3459–3462 (2009)
18. Shi, D.Q., Ko, R.K., Song, K.J., Chung, J.K., Choi, S.J., Park, Y.M., Shin, K.C., Yoo, S.I., Park, C.: Effects of deposition rate and thickness on the properties of YBCO films deposited by pulsed laser deposition. Supercond. Sci. Technol. **17**, S42–S45 (2004)
19. Mogro-Campero, A., Turner, L.G., Hall, E.L.: Large differences of critical current density in thin films of superconducting $YBa_2Cu_3O_{7-x}$. J. Appl. Phys. **65**, 4951–4954 (1989)
20. Luo, L., Wu, X.D., Dye, R.C., Muenchausen, R.E., Foltyn, S.R., Coulter, Y., Maggiore, C.J.: *a*-axis oriented $YBa_2Cu_3O_{7-x}$ thin films on Si with CeO_2 buffer layers. Appl. Phys. Lett. **59**, 2043–2045 (1991)
21. Matias, V., Hänisch, J., Reagor, D., Rowley, E.J., Sheehan, C.: Reactive co-evaporation of YBCO as a low-cost process for fabricating coated conductors. IEEE Trans. Appl. Supercond. **19**, 3172–3175 (2009)
22. Zhou, H., Maiorov, B., Baily, S.A., Dowden, P.C., Kennison, J.A., Stan, L., Holesinger, T.G., Jia, Q.X., Foltyn, S.R., Civale, L.: Thickness dependence of critical current density in $YBa_2Cu_3O_{7-\delta}$ films with $BaZrO_3$ and Y_2O_3 addition. Supercond. Sci. Technol. **22**, 085013 (2009)
23. Rupich, M.W., Li, X., Sathyamurthy, S., Thieme, C.L.H., DeMoranville, K., Gannon, J., Fleshler, S.: Second generation wire development at AMSC. IEEE Trans. Appl. Supercond. **23**, 6601205 (2013)
24. Xiao, G.N., Liu, L.F., Xu, D., Wu, X., Luo, Q., Li, Y.J.: Effects of YSZ buffer layer burface morphology on superconducting performance of YBCO films deposited by pulsed laser deposition on NiW tapes. J. Phys.: Conf. Ser. **507**, 022046 (2014)